

Temperature dependence of spin-polarized transport in ferromagnet / unconventional superconductor junctions

T. Hirai^{1,2}, Y. Tanaka^{1,2}, N. Yoshida³, Y. Asano⁴, J. Inoue¹ and S. Kashiwaya^{2,5}

¹ *Department of Applied Physics, Nagoya University, Nagoya, 464-8603, Japan*

² *CREST Japan Science and Technology Cooperation (JST) 464-8603, Japan*

³ *Department of Microelectronics and Nanoscience, School of Physics and Engineering Physics, Chalmers University of Technology and Goteborg University, S-412 96 Goteborg, Sweden*

⁴ *Department of Applied Physics, Hokkaido University, Sapporo 060-8628, Japan*

⁵ *National Institute of Advanced Industrial Science and Technology, Tsukuba, 305-8568, Japan*

(Dated: October 29, 2018)

Tunneling conductance in ferromagnet / unconventional superconductor junctions is studied theoretically as a function of temperatures and spin-polarization in ferromagnets. In d -wave superconductor junctions, a zero-energy Andreev bound state drastically affects the temperature dependence of the zero-bias conductance (ZBC). In p -wave superconductor junctions, numerical results show various temperature dependence of the ZBC depending on the direction of the magnetic moment in ferromagnets and the pairing symmetry in superconductors such as p_x , p_y and $p_x + ip_y$ -wave symmetries. The last one is a candidate for the pairing symmetry of Sr_2RuO_4 . From these characteristic features in the conductance, we may obtain the information about the degree of spin-polarization in ferromagnets and the direction of the d -vector in spin-triplet superconductors.

I. INTRODUCTION

In recent years, transport properties in unconventional superconductor junctions have been studied both theoretically and experimentally. In these junctions, a zero energy state (ZES)^{1,2,3} formed at the junction interface plays an important role in the tunneling spectroscopy. It is now well known the ZES is responsible for zero-bias conductance peak (ZBCP) in the high- T_C superconductor junctions^{4,5,6,7,8,9} and related phenomena^{10,11,12,13,14,15,16,17,18,19,20,21}. The theoretical studies clearly relate the formation of the ZES to the ZBCP in tunneling spectroscopy^{22,23,24,25}. Since the formation of the ZES is a general phenomenon in unconventional superconductor junctions, the ZBCP is also expected in spin-triplet superconductor junctions^{26,27,28,29,30,31,32}. Actually, the ZBCP has been observed in junctions of Sr_2RuO_4 ^{33,34} and UBe_{13} ³⁵. The ZBCP has also been theoretically predicted for organic superconductors $(\text{TMTSF})_2\text{X}$ very recently^{36,37,38}.

From a view of future device application, transport properties in hybrid structures consist of ferromagnets and superconductors have attracted much attention. It was pointed out in ferromagnet / insulator / spin-singlet unconventional superconductor (F/I/S) junctions that the amplitude of the ZBCP decreases with increasing the magnitude of the exchange potential in ferromagnets. This is because the exchange potential breaks the time-reversal symmetry and suppresses the retro-reflectivity of the Andreev reflection^{39,40,41,42,43,44,45,46,49,50}. Thus the ZBCP is sensitive to the degree of spin-polarization in ferromagnets. Since the tunneling conductance is independent of the magnitude of the insulating barrier⁵¹, it is possible to estimate the spin-polarization in ferromagnets through the temperature dependence of the ZBCP. An experimental test would be carried out in $\text{La}_{0.7}\text{Sr}_{0.3}\text{MnO}_3/\text{YBa}_2\text{Cu}_3\text{O}_{7-x}$ junctions in near fu-

ture^{52,53,54,55}.

When spin-triplet superconductors are attached to ferromagnets^{43,44}, the ZBCP depends not only on the spin-polarization also on other parameters such as relative angles between the d -vector in triplet superconductors and the magnetic moment in ferromagnets^{31,32,45,46}. Thus it may be possible to know details of the pair potential by comparing the characteristic feature of the ZBCP in theoretical calculations and those in experiments. For this purpose, it is necessary to know effects of another ingredients such as temperatures and the profile of the pair potential near the junction interface on the ZBCP. It is known that the amplitude of pair potential is drastically suppressed at a surface or a interface of superconductors in the presence of the ZES^{2,28,56,57,58,67}. Although there are several studies on tunneling phenomena in ferromagnet / unconventional superconductor junctions so far^{47,48}, such issues have never been addressed yet.

In this paper, we calculate the tunneling conductance in ferromagnet / unconventional superconductor junctions as a function of temperatures and degrees of spin-polarization in ferromagnets, where the spatial dependence of the pair potential is determined self-consistently based on the quasiclassical Green's function theory. We choose d -wave, and $p_x + ip_y$ -wave symmetries for the pair potentials which are candidates for pairing symmetries of high- T_C cuprates and Sr_2RuO_4 , respectively. For comparison, we also study the conductance in p_x - and p_y -wave superconductor junctions. From the calculated results, we reach the following conclusions.

(1) In d -wave junctions with (110) orientation and p_x -wave junctions, an incident quasiparticle from a ferromagnet always feels the ZES irrespective of the incident angles. The zero-bias tunneling conductance (ZBC) at the zero temperature is insensitive to the barrier potential at the interface. This result indicates a possibility to estimate the magnitude of the spin-polarization of ferro-

magnets at sufficiently low temperatures (T) in experiments.

(2) In d -wave junctions with (110) orientation and p_x -wave junctions, the ZBC monotonically decreases with increasing temperatures for small magnitudes of spin-polarization. On the other hand for large magnitudes of polarization, the ZBC becomes an increasing function of temperatures. While for d -wave junctions with (100) orientation and p_y -wave junctions, where the ZES does not appear, the ZBC is an increasing function of T independent of the spin-polarization. For $p_x + ip_y$ -wave junctions, the ZBC first decreases with increasing T then increases.

(3) For p -wave junctions, the ZBC has various temperature dependence depending on the direction of the magnetic moment in ferromagnets. This unique property is peculiar to spin-triplet superconductors.

(4) Throughout this paper, we calculate the ZBC in two ways; i) the spatial dependence of the pair potential is assumed to be the step function (non-SCF calculation), ii) the spatial depletion of the pair potentials is determined self-consistently (SCF-calculation). By comparing the conductance in the two ways, we found that the results in the non-SCF calculation are qualitatively the same with those in the SCF-calculation.

The organization of this paper is as follows. In Sec. 2, we formulate the tunneling conductance with arbitrary angle between the magnetization axis of the ferromagnet and c -axis of the superconductor. We show the tunneling conductance depends on the direction of the magnetic moments only when superconductors have spin-triplet pairing. In Sec. 3, we calculate the polarization and temperature dependence of ZBC for both d -wave and p -wave junctions. In Sec. 4, we summarize this paper.

II. FORMULATION

Let us consider a two-dimensional F/I/S junction in the clean limit as shown in Fig. 1. We assume a flat interface at $x = 0$. The insulator is described by the delta-function $V(x) = H\delta(x)$, where H represents the strength of the barrier potential. We also assume that the Fermi energy E_F and the effective mass m in the ferromagnet are equal to those in the superconductor. The Stoner model is applied to describe ferromagnets, where the exchange potential U characterizes the ferromagnetism. The wave numbers in the ferromagnet for the majority (\uparrow) and the minority (\downarrow) spins are denoted by $k_{\uparrow(\downarrow)} = \sqrt{\frac{2m}{\hbar^2}(E_F + (-)U)}$. The wave functions $\Psi(\mathbf{r})$ are obtained by solving the Bogoliubov-de Gennes (BdG) equation under the quasiclassical approximation^{59,60}

$$E\Psi(\mathbf{r}) = \int d\mathbf{r}' \tilde{H}(\mathbf{r}, \mathbf{r}')\Psi(\mathbf{r}'), \quad \Psi(\mathbf{r}) = \begin{pmatrix} u_{\uparrow}(\mathbf{r}) \\ u_{\downarrow}(\mathbf{r}) \\ v_{\uparrow}(\mathbf{r}) \\ v_{\downarrow}(\mathbf{r}) \end{pmatrix} \quad (1)$$

$$\tilde{H}(\mathbf{r}, \mathbf{r}') = \begin{pmatrix} \hat{H}(\mathbf{r})\delta(\mathbf{r} - \mathbf{r}') & \hat{\Delta}(\mathbf{r}, \mathbf{r}') \\ \hat{\Delta}^\dagger(\mathbf{r}, \mathbf{r}') & -\hat{H}^*(\mathbf{r})\delta(\mathbf{r} - \mathbf{r}') \end{pmatrix},$$

where E is the energy of a quasiparticle measured from E_F , $\hat{H}(\mathbf{r}) = h_0\hat{\mathbf{1}} - \mathbf{U}(\mathbf{r}) \cdot \boldsymbol{\sigma}(\mathbf{r})$, $h_0 = -\frac{\hbar^2}{2m}\nabla^2 + V(x) - E_F$, $\mathbf{U}(\mathbf{r}) = U\Theta(-x)\mathbf{n}$, $\hat{\mathbf{1}}$ and $\boldsymbol{\sigma}$ are the 2×2 identity matrix and the Pauli matrix, respectively. Here \mathbf{n} points the direction of the magnetic moment in ferromagnets and $\Theta(x)$ is the Heaviside step function. The indices \uparrow and \downarrow denote the spin degree of freedom of a quasiparticle in superconductors. The magnetization axis in ferromagnets is represented in a polar coordinate (θ_M, ϕ_M) as shown in Fig. 1. We assume that the quantization axis of spin in the triplet superconductors is in the c -axis which is parallel to z direction. At first, we assume that the pair potential is a constant independent of x ,

$$\hat{\Delta}(\theta_S, x) = \hat{\Delta}(\theta_S)\Theta(x), \quad (2)$$

where $\hat{\Delta}(\theta_S)$ does not have the spatial dependence, $k_x = k_F \cos\theta_S$ and $k_y = k_F \sin\theta_S$ are the wavenumber in superconductors with k_F being the Fermi wave number. The pair potential $\hat{\Delta}(\theta_S)$ is given by

$$\hat{\Delta}(\theta_S) = \begin{pmatrix} \Delta_{\uparrow\uparrow}(\theta_S) & \Delta_{\uparrow\downarrow}(\theta_S) \\ \Delta_{\downarrow\uparrow}(\theta_S) & \Delta_{\downarrow\downarrow}(\theta_S) \end{pmatrix}. \quad (3)$$

The Hamiltonian in Eq. (2) is written in the coordinate of the spin space in the superconductor. It is comprehensive to rewrite the Hamiltonian in the coordinate of spin space in the ferromagnet since this notation is useful to consider the scattering processes. The Hamiltonian in the coordinate of spin space in the ferromagnet is ob-

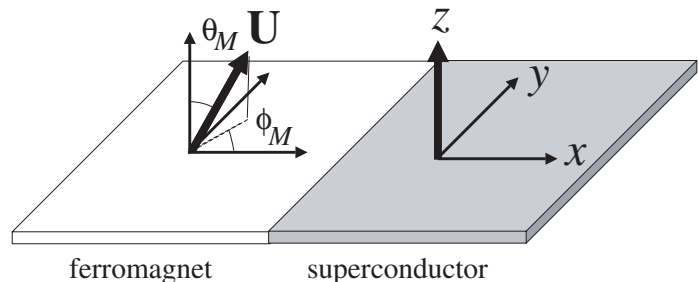


FIG. 1: Schematic illustration of a ferromagnet / superconductor junction. The direction of the magnetization axis is denoted by a polar coordinate (θ_M, ϕ_M) .

tained by using the following unitary transformation:

$$\tilde{H}_F(\mathbf{r}, \mathbf{r}') = \tilde{U}^\dagger \hat{H}(\mathbf{r}, \mathbf{r}') \tilde{U}, \quad (4)$$

$$\tilde{U} = \begin{pmatrix} \hat{U} & 0 \\ 0 & \hat{U}^* \end{pmatrix}, \quad \hat{U} = \begin{pmatrix} \gamma_1 & -\gamma_2^* \\ \gamma_2 & \gamma_1^* \end{pmatrix}, \quad (5)$$

$$\gamma_1 = \cos \frac{\theta_M}{2} e^{-i\phi_M}, \quad \gamma_2 = \sin \frac{\theta_M}{2} e^{i\phi_M}, \quad (6)$$

where \hat{U} is the operator which diagonalizes the $\hat{H}(\mathbf{r})$. The effective pair potential in the coordinate of spin space in ferromagnet is rewritten as

$$\hat{\Delta}^F(\theta_S) = \hat{U}^\dagger \hat{\Delta}(\theta_S) \hat{U}^*. \quad (7)$$

Here, we consider the four types of pair potentials, d -wave, p_x -wave, p_y -wave and $p_x + ip_y$ -wave symmetries in superconductors. In d -wave case, the pair potential is described as

$$\Delta_{\uparrow\downarrow}(\theta_S) = -\Delta_{\downarrow\uparrow}(\theta_S) \equiv \Delta_0 f(\theta_S), \quad (8)$$

$$\Delta_{\uparrow\uparrow}(\theta_S) = \Delta_{\downarrow\downarrow}(\theta_S) = 0, \quad (9)$$

$$f(\theta_S) = \cos[2(\theta_S - \alpha)], \quad (10)$$

where α is the angle between a -axis of the high- T_c superconductors and the interface normal. The effective pair potential in the coordinate of spin space in ferromagnet is given by

$$\hat{\Delta}^F(\theta_S) \equiv \begin{pmatrix} \Delta_{\uparrow\uparrow}^F(\theta_S) & \Delta_{\uparrow\downarrow}^F(\theta_S) \\ \Delta_{\downarrow\uparrow}^F(\theta_S) & \Delta_{\downarrow\downarrow}^F(\theta_S) \end{pmatrix}, \quad (11)$$

$$= \begin{pmatrix} 0 & \Delta_0 f(\theta_S) \\ -\Delta_0 f(\theta_S) & 0 \end{pmatrix}, \quad (12)$$

$$= \hat{\Delta}(\theta_S). \quad (13)$$

As shown in Eq. (13), the expression of the pair potential remains unchanged under the transformation in Eq. (4). Therefore transport properties are expected to be independent of the direction of the magnetic moment. This conclusion can be applied to any spin-singlet superconductors. On the other hand in spin-triplet superconductors, the pair potentials are given by

$$\Delta_{\uparrow\downarrow}(\theta_S) = \Delta_{\downarrow\uparrow}(\theta_S) = \Delta_0 f(\theta_S), \quad (14)$$

$$\Delta_{\uparrow\uparrow}(\theta_S) = \Delta_{\downarrow\downarrow}(\theta_S) = 0, \quad (15)$$

where the direction of the d -vector is parallel to the c -axis and

$$f(\theta_S) = \begin{cases} \cos \theta_S & \text{for } p_x \text{-symmetry,} \\ \sin \theta_S & \text{for } p_y \text{-symmetry,} \\ e^{i\theta_S} & \text{for } p_x + ip_y \text{-symmetry.} \end{cases} \quad (16)$$

Because the spin degree of freedom of Cooper pairs is active in triplet superconductors, the pair potential after the transformation in Eq. (4) depends on the direction of the magnetic moment

$$\hat{\Delta}^F(\theta_S) = \begin{pmatrix} \sin \theta_M & \cos \theta_M \\ \cos \theta_M & -\sin \theta_M \end{pmatrix} f(\theta_S) \Delta_0. \quad (17)$$

There are four reflection processes when an electron with the majority spin is incident from ferromagnets:

- i) Andreev reflection to majority spin ($a_{\uparrow\uparrow}$)
- ii) Andreev reflection to minority spin ($a_{\uparrow\downarrow}$)
- iii) normal reflection to majority spin ($b_{\uparrow\uparrow}$) and
- iv) normal reflection to minority spin ($b_{\uparrow\downarrow}$).

Similar reflection processes are also possible, when an electron with the minority spin is incident from ferromagnets. The Andreev and the normal reflection coefficients are denoted by $a_{\bar{s}\bar{s}'}$ and $b_{\bar{s}\bar{s}'}$, respectively. In these coefficients, a quasiparticle is reflected from the spin-channel \bar{s} into the spin-channel \bar{s}' .

The wave function in ferromagnets for majority spin injection is represented by

$$\begin{aligned} \Psi_{\uparrow}(x) = & e^{ik_{F\uparrow}x} \begin{pmatrix} 1 \\ 0 \\ 0 \\ 0 \end{pmatrix} + a_{\uparrow\uparrow} e^{ik_{F\uparrow}x} \begin{pmatrix} 0 \\ 0 \\ 1 \\ 0 \end{pmatrix} + a_{\uparrow\downarrow} e^{ik_{F\downarrow}x} \\ & \times \begin{pmatrix} 0 \\ 0 \\ 0 \\ 1 \end{pmatrix} + b_{\uparrow\uparrow} e^{-ik_{F\uparrow}x} \begin{pmatrix} 1 \\ 0 \\ 0 \\ 0 \end{pmatrix} + b_{\uparrow\downarrow} e^{-ik_{F\downarrow}x} \begin{pmatrix} 0 \\ 1 \\ 0 \\ 0 \end{pmatrix}, \end{aligned} \quad (18)$$

where $k_{F\downarrow} < k_S < k_{F\uparrow}$ and $k_S \approx \sqrt{\frac{2mE_F}{\hbar^2}}$. The wave function for minority spin injection is written in the similar way. The coefficients $a_{\bar{s}\bar{s}'}$ and $b_{\bar{s}\bar{s}'}$ are determined by solving the BdG equation with the quasiclassical approximation under appropriate boundary conditions.

The tunneling conductance σ_T (eV) for finite temperature is given by^{61,62,63}

$$\sigma_T(eV) = \frac{2e^2}{h} G, \quad (19)$$

$$\begin{aligned} G = & \frac{1}{16k_B T} \int_{-\infty}^{\infty} dE \int_{-\pi/2}^{\pi/2} d\theta_S \cos \theta_S \\ & \times (\sigma_{S\uparrow}(\theta_S) + \sigma_{S\downarrow}(\theta_S)) \operatorname{sech}^2 \left(\frac{E - eV}{2k_B T} \right), \end{aligned} \quad (20)$$

$$\begin{aligned} \sigma_{S\uparrow} = & 1 + |a_{\uparrow\uparrow}|^2 - |b_{\uparrow\uparrow}|^2 + \left(\frac{\eta_{\downarrow}}{\eta_{\uparrow}} |a_{\uparrow\downarrow}|^2 - \frac{\eta_{\downarrow}}{\eta_{\uparrow}} |b_{\uparrow\downarrow}|^2 \right) \\ & \times \Theta(\theta_C - |\theta_S|), \end{aligned} \quad (21)$$

$$\begin{aligned} \sigma_{S\downarrow} = & \left(1 + \frac{\eta_{\uparrow}}{\eta_{\downarrow}} |a_{\downarrow\uparrow}|^2 + |a_{\downarrow\downarrow}|^2 - \frac{\eta_{\uparrow}}{\eta_{\downarrow}} |b_{\downarrow\uparrow}|^2 - |b_{\downarrow\downarrow}|^2 \right) \\ & \times \Theta(\theta_C - |\theta_S|), \end{aligned} \quad (22)$$

with $Z_{\theta_S} = Z / \cos \theta_S$, $Z = 2mH/\hbar^2 k_F$ and $\eta_{\uparrow(\downarrow)} = \sqrt{1 \pm X / \cos^2 \theta_S}$. Here $X = U/E_F$ is defined as the spin-polarization parameter. The quantity $\sigma_{S\uparrow(\downarrow)}$ is the tunneling conductance for an incident electron with the majority (minority) spin. For $|\theta_S| > \theta_C = \cos^{-1} \sqrt{X}$, the reflected wave becomes an evanescent wave and does not contribute to the tunneling conductance. As shown in

above equations, the tunneling conductance depends on θ_M only when superconductors have spin-triplet Cooper pairs. The tunneling conductance can be summarized in simple equations in following several cases. When θ_M is 0 or π in spin-triplet superconductors, the conductance is described by

$$\sigma_{S\uparrow} = \sigma_{N\uparrow}(A + B), \quad (23)$$

$$\sigma_{S\downarrow} = \sigma_{N\downarrow}C \quad (24)$$

$$A = [1 - |\Gamma_+\Gamma_-|^2(1 - \sigma_{N\downarrow}) + \sigma_{N\downarrow}|\Gamma_+|^2] \times \Theta(\theta_C - |\theta_S|)/L_{D1}, \quad (25)$$

$$B = 1 - \Theta(\theta_C - |\theta_S|)[1 - |\Gamma_+\Gamma_-|^2]/L_{D1}, \quad (26)$$

$$C = [1 - |\Gamma_+\Gamma_-|^2(1 - \sigma_{N\uparrow}) + \sigma_{N\uparrow}|\Gamma_+|^2] \times \Theta(\theta_C - |\theta_S|)/L_{D2}, \quad (27)$$

$$L_{D1} = \left| 1 - \Gamma_+\Gamma_- \sqrt{1 - \sigma_{N\downarrow}} \sqrt{1 - \sigma_{N\uparrow}} \right. \\ \left. \times \exp[i(\varphi_{\downarrow} - \varphi_{\uparrow})] \right|^2, \quad (28)$$

$$L_{D2} = \left| 1 - \Gamma_+\Gamma_- \sqrt{1 - \sigma_{N\downarrow}} \sqrt{1 - \sigma_{N\uparrow}} \right. \\ \left. \times \exp[i(\varphi_{\uparrow} - \varphi_{\downarrow})] \right|^2, \quad (29)$$

with

$$\exp(i\varphi_{\downarrow}) = \frac{1 - \eta_{\downarrow} + iZ\theta_S}{\sqrt{1 - \sigma_{N\downarrow}}(1 + \eta_{\downarrow} - iZ\theta_S)}, \quad (30)$$

$$\exp(-i\varphi_{\uparrow}) = \frac{1 - \eta_{\uparrow} - iZ\theta_S}{\sqrt{1 - \sigma_{N\uparrow}}(1 + \eta_{\uparrow} - iZ\theta_S)}. \quad (31)$$

Above equations can be applied to the spin-singlet superconductors. When $\theta_M = \pi/2$ in spin-triplet superconductors, the conductance for each spin is given by

$$\sigma_{S\uparrow} = \sigma_{N\uparrow} \frac{1 - |\Gamma_+\Gamma_-|^2(1 - \sigma_{N\uparrow}) + \sigma_{N\uparrow}|\Gamma_+|^2}{|1 - \Gamma_+\Gamma_-(1 - \sigma_{N\uparrow})|^2}, \quad (32)$$

$$\sigma_{S\downarrow} = \sigma_{N\downarrow} \frac{1 - |\Gamma_+\Gamma_-|^2(1 - \sigma_{N\downarrow}) + \sigma_{N\downarrow}|\Gamma_+|^2}{|1 - \Gamma_+\Gamma_-(1 - \sigma_{N\downarrow})|^2} \\ \times \Theta(\theta_C - |\theta_S|). \quad (33)$$

In above equations, we define

$$\Gamma_{\pm} = \pm \frac{E - \sqrt{E^2 - |\Delta(\theta_S)|^2}}{\Delta(\theta_S)^*}, \quad (34)$$

$$\sigma_{N\uparrow} = \frac{4\eta_{\uparrow}}{(1 + \eta_{\uparrow})^2 + Z_{\theta_S}^2}, \quad (35)$$

$$\sigma_{N\downarrow} = \frac{4\eta_{\downarrow}}{(1 + \eta_{\downarrow})^2 + Z_{\theta_S}^2} \Theta(\theta_C - |\theta_S|). \quad (36)$$

In this paper, the dependence of the pair potential on temperatures is described by the BCS's gap equation. The spatial dependence of the pair potential can be described by $\hat{\Delta}(\theta_S, x)$ with $\hat{\Delta}(\theta_S, x) = \bar{\Delta}(\theta_S, x)\Theta(x)$. In order to determine the spatial dependence of $\hat{\Delta}(\theta_S, x)$,

we apply the quasiclassical Green's function theory developed by Hara, Nagai, et. al.^{2,58,64,65}. In the following, we briefly explain the method in the case of spin-singlet superconductors. An extension to spin-triplet superconductors is straightforward. The spatial dependence of $\hat{\Delta}(\theta_S, x)$ is calculated by the diagonal elements of the matrix Green function $g_{\alpha\alpha}(x)$ which are represented by

$$g_{++}(\theta_S, x) = i \begin{pmatrix} \frac{1+D_+(x)F_+(x)}{1-D_+(x)F_+(x)} & \frac{2iF_+(x)}{1-D_+(x)F_+(x)} \\ \frac{2iD_+(x)}{1-D_+(x)F_+(x)} & -\frac{1+D_+(x)F_+(x)}{1-D_+(x)F_+(x)} \end{pmatrix}, \quad (37)$$

$$g_{--}(\theta_S, x) = i \begin{pmatrix} \frac{1+D_-(x)F_-(x)}{-1+D_-(x)F_-(x)} & \frac{2iF_-(x)}{-1+D_-(x)F_-(x)} \\ \frac{2iD_-(x)}{-1+D_-(x)F_-(x)} & -\frac{1+D_-(x)F_-(x)}{-1+D_-(x)F_-(x)} \end{pmatrix}, \quad (38)$$

where an index $\alpha = \pm$ specifies the direction of the momentum in the x direction. In these Green functions, $D_{\alpha}(x)$ and $F_{\alpha}(x)$ obey the following equations

$$\hbar|v_{Fx}|D_{\alpha}(x) = \alpha \\ \times [2\omega_m D_{\alpha}(x) + \bar{\Delta}(\theta_S, x)D_{\alpha}^2(x) - \bar{\Delta}^*(\theta_S, x)], \quad (39)$$

$$\hbar|v_{Fx}|F_{\alpha}(x) = \alpha \\ \times [-2\omega_m F_{\alpha}(x) + \bar{\Delta}^*(\theta_S, x)F_{\alpha}^2(x) - \bar{\Delta}(\theta_S, x)], \quad (40)$$

$$\hat{\Delta}(\theta_S, x) = \begin{pmatrix} 0 & \bar{\Delta}(\theta_S, x) \\ -\bar{\Delta}(\theta_S, x) & 0 \end{pmatrix}. \quad (41)$$

The boundary conditions at the interface are given by^{66,67}

$$F_+(0) = \frac{(\eta_{\uparrow} - 1 + iZ)(\eta_{\downarrow} - 1 - iZ)}{(\eta_{\uparrow} + 1 + iZ)(\eta_{\downarrow} + 1 - iZ)} D_-(0)^{-1}, \quad (42)$$

$$F_-^{-1}(0) = \frac{(\eta_{\uparrow} - 1 + iZ)(\eta_{\downarrow} - 1 - iZ)}{(\eta_{\uparrow} + 1 + iZ)(\eta_{\downarrow} + 1 - iZ)} D_+(0). \quad (43)$$

We first solve $D_{\pm}(x)$ and $F_{\pm}(x)$ in Eqs. (39) and (40), then calculate $g_{\pm,\pm}(\theta, x)$ in Eqs. (37) and (38) for a given $\bar{\Delta}(\theta_S, x)$. By using $g_{\pm,\pm}(\theta, x)$, $\hat{\Delta}(\theta_S, x)$ is given by the following equations

$$\hat{\Delta}(\theta_S, x) = \sum_{n\alpha} \int_{\pi/2}^{\pi/2} d\theta_S' V(\theta_S, \theta_S') g_{\alpha,\alpha}(\theta_S', x), \quad (44)$$

$$V(\theta, \theta') = g_0 f(\theta) f(\theta'), \quad (45)$$

$$g_0 = \frac{2\pi k_B T}{\ln(T/T_C) + \sum_{0 < m < m_a} \frac{1}{m+1/2}}, \quad (46)$$

where we introduce the cut-off m_a to regularize g_0 and $f(\theta)$ is given in Eqs. (10) and (16). The iteration is carried out until the sufficient convergence is obtained. In this way, we obtain $\bar{\Delta}(\theta, x)$, i.e., $\hat{\Delta}(\theta, x)$ self-consistently.

Under the pair potential in the self-consistent calculation, we obtain $\check{\Gamma}_{\pm}(x)$ by solving

$$i\hbar|v_{Fx}|\check{\Gamma}_+(x) \\ = \alpha [2E\check{\Gamma}_+(x) - \bar{\Delta}(\theta_S, x)\check{\Gamma}_+^2(x) - \bar{\Delta}^*(\theta_S, x)], \quad (47)$$

$$i\hbar|v_{Fx}|\check{\Gamma}_-(x) \\ = \alpha [2E\check{\Gamma}_-(x) - \bar{\Delta}^*(\theta_S, x)\check{\Gamma}_-^2(x) - \bar{\Delta}(\theta_S, x)]. \quad (48)$$

By substituting Γ_{\pm} into Eqs. (23)-(34), we can calculate the tunneling conductance. In what follows, we assume that the transition temperature of ferromagnets is much larger than T_C which is the transition temperature of superconductors. In such situation, we can neglect the temperature dependence of X .

III. RESULTS

A. polarization dependence of zero-bias conductance

In this subsection, we show calculated results of the ZBC at the zero temperature as a function of the spin-polarization in ferromagnets (X). The dimensionless ZBC (Γ) is given by

$$\Gamma = \frac{\sigma_T(0)h}{2e^2}. \quad (49)$$

At first we show the conductance obtained in the step-function model, where the spatial dependence of the pair potential is not determined self-consistently (non-SCF calculation). The X -dependence of Γ at the zero temperature for d -wave junctions is plotted in Fig. 2. The magnitude of Γ is always a decreasing function of X . For $\alpha = 0$ (Fig. 2(a)), Γ decreases with increasing of X . On the other hand, for $\alpha = \pi/4$ (Fig. 2(b)), Γ is completely independent of Z because of the perfect Andreev reflection due to the zero-energy resonance state at the interface.

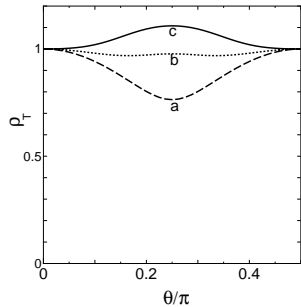


FIG. 2: X dependence of the zero-bias conductance Γ in non-SCF calculation for (a) $\alpha = 0$ and (b) $\alpha = \pi/4$ in d -wave junctions at zero temperature. a: $Z = 0$, b: $Z = 1$ and c: $Z = 5$.

Secondly, we show the polarization dependence of Γ in triplet p_x , p_y and $p_x + ip_y$ -wave superconductor junctions as shown in Fig. 3, where the pair potential are given in Eqs. (14), (15) and (16). The conductance depends on θ_M for all pairing symmetries. The spin degree of freedom remains in spin-triplet superconductors. As a consequence, the conductance depends on the relative angle between the magnetic moment in ferromagnets and d -vector in superconductor. This is the characteristic feature of p -wave junctions. For $\theta_M = 0$, as shown

in Figs. 3 (a), (d), and (g), Γ approaches to zero in the limit of $X \rightarrow 1$ independent of Z . In these cases, the diagonal elements in Eq. (3) disappear and a quasiparticle suffers the spin-flip in the Andreev reflection, (i.e., $a_{\uparrow,\uparrow} = a_{\downarrow,\downarrow} = 0$). For $|\theta_S| > \theta_C$, the Andreev reflection to \downarrow spin becomes the evanescent wave. At the same time, an incident wave with \downarrow spin vanishes. Thus Γ vanishes in the limit of $X = 1$, where ferromagnets are referred to as half-metals. On the other hand, for $\sin\theta_M \neq 0$, Γ takes finite values even in $X \rightarrow 1$ as shown in Figs. 3 (b) (c), (e) (f) (h), and (i) because the spin-conserved Andreev reflection is still possible in these junctions. The results for $\theta_M = \pi/2$ are shown in Figs. 3 (c) (f) and (i). In this case, the off-diagonal elements in Eq. (17) become zero. Thus spin of a quasiparticle is conserved in the Andreev reflection, (i.e., $a_{\uparrow,\downarrow} = a_{\downarrow,\uparrow} = 0$). The Andreev reflection of an electron with \uparrow spin survives irrespective of θ_S , whereas that of an electron with \downarrow spin vanishes for $|\theta_S| > \theta_C$. We note in p_x -wave junctions that Γ does not depend on Z as well as d -wave junctions with $\alpha = \pi/4$. This is because the ZES's are formed at the interface.

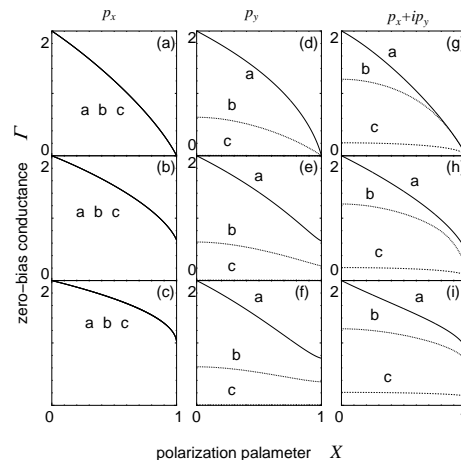


FIG. 3: X dependence of Γ in non-SCF calculation. (a) $\theta_M = 0$, (b) $\theta_M = \pi/4$ and (c) $\theta_M = \pi/2$ for p_x -wave junctions. (d) $\theta_M = 0$, (e) $\theta_M = \pi/4$ and (f) $\theta_M = \pi/2$ for p_y -wave junctions. (g) $\theta_M = 0$, (h) $\theta_M = \pi/4$ and (i) $\theta_M = \pi/2$ for $p_x + ip_y$ -wave junctions. a: $Z = 0$, b: $Z = 1$ and c: $Z = 5$.

Thirdly we show the tunneling conductance under the pair potential whose spatial dependence is determined self-consistently (SCF calculation). The results for d , p_x , p_y , and $p_x + ip_y$ -wave junctions are shown in Figs. 4 and 5. The conductance in SCF calculation in Figs. 4 and 5 should be compared with corresponding results in non-SCF calculation in Figs. 2 and 3, respectively. We do not find any remarkable differences between the results in SCF calculation and those in non-SCF calculation as shown in these figures.

Finally, X dependence of Γ is plotted for various temperatures. As seen from Fig. 2(b), using tunneling through ZES, we can determine the magnitude of X through the value of Γ . This is a unique property for d -

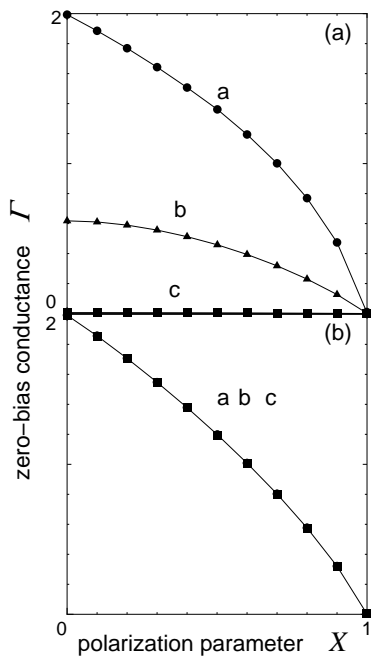


FIG. 4: X dependence of Γ in SCF calculation for d -wave junctions. (a) $\alpha = 0$ and (b) $\alpha = \pi/4$. a: $Z = 0$, b: $Z = 1$ and c: $Z = 5$.

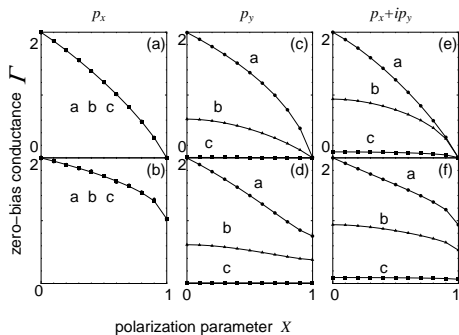


FIG. 5: X dependence of Γ in SCF calculation. (a) $\theta_M = 0$ and (b) $\theta_M = \pi/2$ with p_x -wave junctions. (c) $\theta_M = 0$ and (d) $\theta_M = \pi/2$ with p_y -wave junctions. (e) $\theta_M = 0$ and (f) $\theta_M = \pi/2$ with $p_x + ip_y$ -wave junctions. a: $Z = 0$, b: $Z = 1$ and c: $Z = 5$.

wave superconductor with $\alpha = \pi/4$, or p -wave junctions where all quasiparticles feel ABS independent of their directions of motions. Since Γ is plotted at zero temperature in Fig. 2(b), it is actually important how this property holds even in finite temperatures. As shown in Fig. 6, when the magnitude of the temperature T is sufficiently smaller than T_C , Γ is almost insensitive to the magnitude of Z and we can estimate the magnitude of X through Γ . In the actual experiments, high T_C cuprates, *e.g.*, YBaCuO, BiSrCaCuO, with (110) oriented interface is a promising candidate. In such a case, the actual value of $0.001T_C$ becomes 0.1K and this temperature is fully

accessible in the experiments.

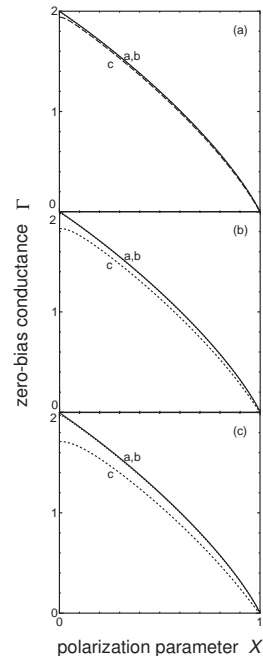


FIG. 6: X dependence of Γ for various temperatures for d -wave junctions for $\alpha = \pi/4$ in non SCF calculation. (a) $T/T_C = 0.001$, (b) $T/T_C = 0.005$ and (c) $T/T_C = 0.01$. a: $Z = 0$, b: $Z = 1$ and c: $Z = 5$.

B. Temperature dependence of zero-bias conductance

In this subsection, we discuss the temperature dependence of Γ . In the first part, we show the conductance in the non-SCF calculation. Then the results are compared with those in the SCF calculation in the second part. At first let us focus on d -wave junctions for $\alpha = 0$ as shown in Figs. 7 (a), (b), (c), where the conductance is plotted as a function of temperatures for several magnitudes of the exchange potential X . We note in these junctions that the ZES is not formed at the interface. For $Z = 0$ (see Fig. 7(a)), the exchange potential in ferromagnets significantly affects the temperature-dependence of Γ . For large X , Γ increases with the increase of T as shown in the curve d in Fig. 7(a). The Andreev reflection (two-electron process) is suppressed by the large exchange potential and the current is mainly carried by single electron process. While for small X , Γ decreases with the increase of T as shown in curve a in Fig. 7(a). This is

because the current at the zero-voltage is mainly carried by two-electron process through the Andreev reflection and the amplitude of the Andreev reflection is suppressed for $T \rightarrow T_C$. For $Z = 5$ (Fig. 7(c)), Γ becomes small around $T \sim 0$ because the insulating barrier suppresses the Andreev reflection. The results show that Γ increases monotonically with increasing temperatures independent of X since the current is mainly carried by single electron process. For $Z = 1$ (Fig. 7(b)), excepting for large X , the magnitude of Γ has a non-monotonic temperature dependence, since the amplitude of single-electron process (Andreev reflection) is enhanced (suppressed) with the increase of T .

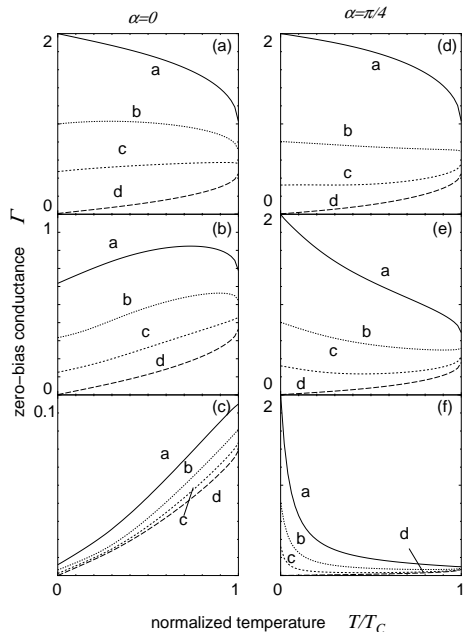


FIG. 7: Temperature dependence of Γ in non-SCF calculation for d -wave junctions. (a) $Z = 0$, (b) $Z = 1$ and (c) $Z = 5$ with $\alpha = 0$. (d) $Z = 0$, (e) $Z = 1$ and (f) $Z = 5$ with $\alpha = \pi/4$. a: $X = 0$, b: $X = 0.7$, c: $X = 0.9$ and d: $X = 0.999$.

Secondly we show the temperature dependence of Γ in d -wave junctions with $\alpha = \pi/4$ in Figs. 7(d), (e), and (f). For $Z = 0$, the line shape of the all curves in Fig. 7(d) are qualitatively similar to those with $\alpha = 0$ shown in Fig. 7(a) since ZES is not formed at the interface. We note in Figs. 7 (d), (e) and (f) that Γ at the zero temperature is independent of Z . The Andreev reflection is perfect in the limit of $Z = 0$. For finite Z , the ZES is formed at the interface which also leads to the perfect Andreev reflection at $T = 0$. The characteristic behavior of the resonant tunneling can be seen in the conductance for large Z . The amplitude of Γ is proportional to the inverse of T for intermediate temperatures (curve a in Fig. 7 (f)). Since the retro-reflectivity of Andreev reflection is broken by the exchange potentials, the degree of the resonance at the interface is weakened. As a results, the temperature dependence deviates from the inverse of T

in curbs b, c and d in Fig. 7 (f). For sufficiently large magnitudes of X , Γ becomes an increasing function of T for $T > 0.5T_C$ as shown in Fig. 7(f). In the case of the d -wave with $\alpha = \pi/4$, we can estimate the magnitude of X from the temperature dependence of Γ .

Thirdly we show temperature dependence of Γ in p_x -wave junctions with $\theta_M = 0$ in Figs. 8(a), (b), (c) and those with $\pi/2$ in Figs. 9(a), (b), (c). As shown in Figs. 8(a), (b) (c), the temperature dependences of Γ are very similar to those of d -wave junctions with $\alpha = \pi/4$. When $\theta_M = 0$, Γ for small X is a decreasing function of T , whereas Γ for large X is an increasing function of T . In the case of $\theta_M = \pi/2$, however, Γ becomes a monotonic decreasing function of T independent of Z as shown in Figs. 9(a), (b), (c). The spin of a quasiparticle is always conserved in the Andreev reflection in this case. Therefore the suppression of the conductance due to the breakdown of the retro-reflectivity becomes weaker than that in the case of $\theta_M = 0$.

Next we show the conductance in p_y -wave junctions with $\theta_M = 0$ in Figs. 8(d), (e), (f) and those with $\pi/2$ in Figs. 9(d), (e), (f). In $\theta_M = 0$, the temperature dependence of Γ are similar to those of d -wave junctions with $\alpha = 0$ shown in Figs. 7(a),(b),(c). In these junctions, no ZES is expected at the interface. In $\theta_M = \pi/2$ as shown in Figs. 9(d), (e), (f), Γ for large X are larger than those with $\theta_M = 0$ in low temperatures. In the case of $\theta_M = \pi/2$, the spin of a quasiparticle is conserved in the Andreev reflection, therefore, the suppression of conductance due to the breakdown of retro-reflectivity becomes weaker than that in the case of $\theta_M = 0$.

Finally we show the conductance in $p_x + ip_y$ -wave junctions with $\theta_M = 0$ in Figs. 8(g), (h), (i) and those with $\pi/2$ in Figs. 9(g), (h), (i). In $p_x + ip_y$ -wave junctions with $\theta_M = 0$, the temperature dependence of Γ can be understood by the combination of the results in p_x -wave and those in p_y -wave junctions because the ZES is only expected for a quasiparticle incident perpendicular to the interface³². As seen from Fig. 8 (g) for $Z=0$, there is no clear difference between Γ in $p_x + ip_y$ -wave junctions with $\theta_M = 0$ and corresponding results in p_x or p_y -wave junctions shown in Figs. 8(a) and (d). For a finite barrier potential at $Z = 1$, the line shape of the all curves in Fig. 8(h) is rather similar to corresponding results in the p_x -wave junctions than those in the p_y -wave junctions. However, Γ are smaller than those in the p_x -wave junctions. For $Z = 5$, Γ for small X are enhanced at low temperatures because of the ZES [see curve a in Fig. 8(i)]. On the other hand, for large X , Γ is an increasing function of T [see curve d in Fig. 8(i)]. For $\theta_M = \pi/2$, Γ becomes a decreasing function of T for all cases as shown in Figs. 9(g), (h), (i). These features are similar to those in the p_x -wave junctions.

It is important to check how the above results are modified in the presence of the spatial dependence in the pair potential near the interface. We show the conductance in SCF calculation in the second part of this subsection. In what follows, we consider two cases of X , $X = 0$ (curve

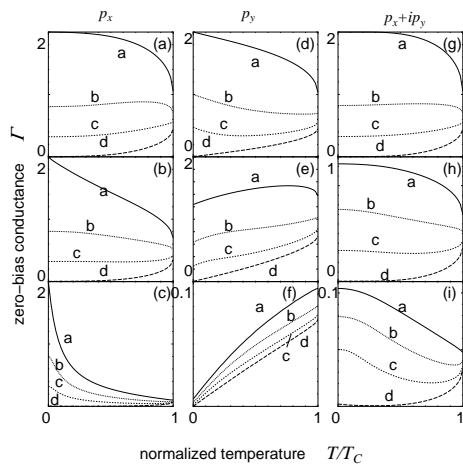


FIG. 8: Temperature dependence of Γ in non-SCF calculation for $\theta_M = 0$. (a) $Z = 0$, (b) $Z = 1$ and (c) $Z = 5$ in p_x -wave junctions. (d) $Z = 0$, (e) $Z = 1$ and (f) $Z = 5$ in p_y -wave junctions. (g) $Z = 0$, (h) $Z = 1$ and (i) $Z = 5$ in $p_x + ip_y$ -wave junctions. a: $X = 0$, b: $X = 0.7$, c: $X = 0.9$ and d: $X = 0.999$.

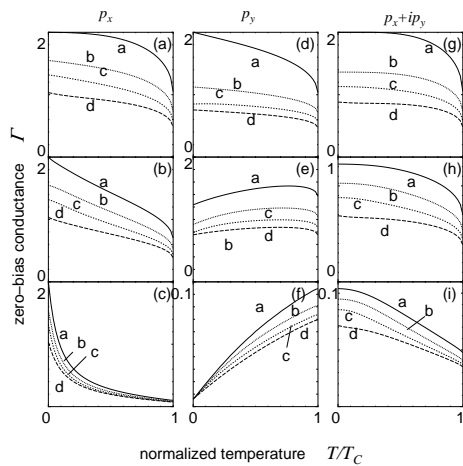


FIG. 9: Temperature dependence of Γ in non-SCF calculation for $\theta_M = \pi/2$. (a) $Z = 0$, (b) $Z = 1$ and (c) $Z = 5$ in p_x -wave junctions. (d) $Z = 0$, (e) $Z = 1$ and (f) $Z = 5$ in p_y -wave junctions. (g) $Z = 0$, (h) $Z = 1$ and (i) $Z = 5$ in $p_x + ip_y$ -wave junctions. a: $X = 0$, b: $X = 0.7$, c: $X = 0.9$ and d: $X = 0.999$.

a) and $X = 0.9$ (curve b). The corresponding results in non-SCF calculation are curves a ($X=0$) and c ($X=0.9$) from Figs. 7 to 9.

In Fig. 10, we show the conductance in SCF calculation in the d -wave junctions with $\alpha = 0$ and $\pi/4$. It is found that the temperature dependences of Γ with $\alpha = 0$ in the SCF calculation are very similar to those in the non-SCF calculation when we compare the results in Figs. 7(a), (b), (c) with those in Figs. 10(a), (b), (c). The same tendency can be seen between the results the d -wave junctions with $\alpha = \pi/4$ in Figs. 7 (d), (e), (f) and those in

Figs. 10(d), (e), (f). When the ZES are formed at the interface, the profile of the pair potential significantly deviates from the step-function. The characteristic behavior of the conductance in the SCF, however, is qualitatively the same with those in the no-SCF. From the calculated results, we conclude that the conductance is insensitive to the profile of the pair potential. This is because the resonant tunneling through the ZES dominates the conductance. We note that the ZES is a consequence of the sign-change of the pair potential.

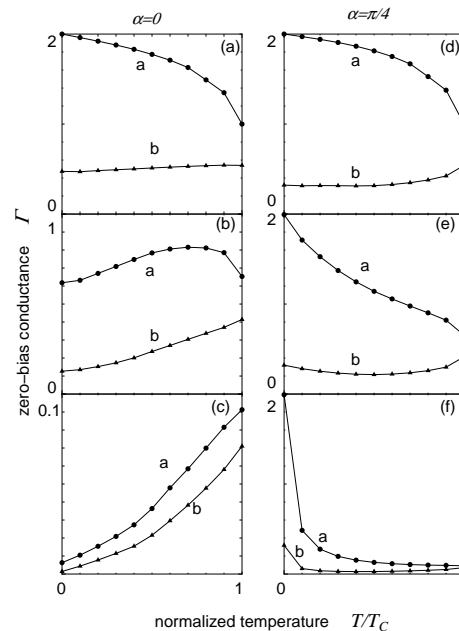


FIG. 10: Temperature dependence of Γ in SCF calculation for d -wave junctions. (a) $Z = 0$, (b) $Z = 1$ and (c) $Z = 5$ with $\alpha = 0$. (d) $Z = 0$, (e) $Z = 1$ and (f) $Z = 5$ for $\alpha = \pi/4$. a: $X = 0$ and b: $X = 0.9$.

In the p_x -wave junctions, line shapes of Γ for $\theta_M = 0$ shown in Figs. 11(a), (b), (c) are very similar to those in the d -wave junctions with $\alpha = \pi/4$. For $\theta_M = \pi/2$, as shown in Figs. 12(a), (b), (d), the magnitudes of Γ are slightly larger than those in Figs. 11(a), (b), (c). These features are almost similar to those found in non-SCF calculation in Figs. 8(a), (b), (c) and Figs. 9(a), (b), (c).

As well as in the p_x -wave junctions, the characteristic behavior of Γ in SCF results in p_y -wave junctions shown in Figs. 11(d), (e), (f) and Figs. 12(d), (e), (f) are almost the same with those obtained in non-SCF calculation shown in Figs. 8(d), (e), (f) and Figs. 9(d), (e), (f).

In the case of $p_x + ip_y$ -wave symmetry, the line-shapes of Γ for (g), (h) and (i) in Figs. 11 and 12 are similar to those in non-SCF results shown in (g) and (h) in Figs. 8 and 9. However, the temperature dependencies of Γ based on the SCF calculation deviate from those in the non-SCF one for large Z [Fig. 11(i) and Fig. 12(i)]. In the SCF calculation, Γ first decreases with the increase of T then increases. The decreasing part is similar to that

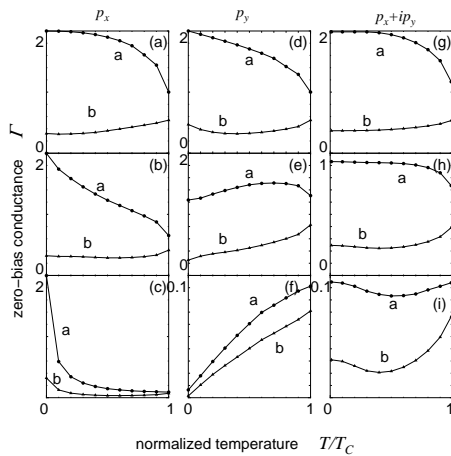


FIG. 11: Temperature dependence of Γ in SCF calculation for $\theta_M = 0$. (a) $Z = 0$, (b) $Z = 1$ and (c) $Z = 5$ in p_x -wave junctions. (d) $Z = 0$, (e) $Z = 1$ and (f) $Z = 5$ in p_y -wave junctions. (g) $Z = 0$, (h) $Z = 1$ and (i) $Z = 5$ in $p_x + ip_y$ -wave junctions. a: $X = 0$ and b: $X = 0.9$.

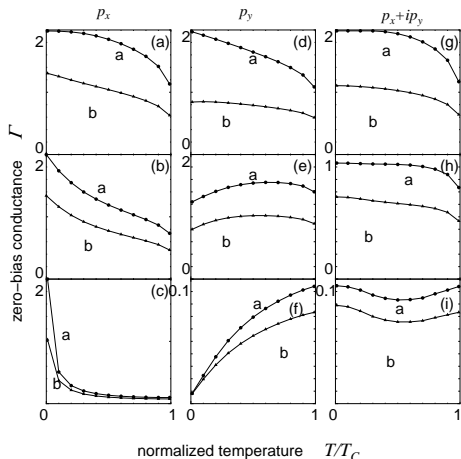


FIG. 12: Temperature dependence of Γ in non-SCF calculation for $\theta_M = \pi/2$. (a) $Z = 0$, (b) $Z = 1$ and (c) $Z = 5$ in p_x -wave junctions. (d) $Z = 0$, (e) $Z = 1$ and (f) $Z = 5$ in p_y -wave junctions. (g) $Z = 0$, (h) $Z = 1$ and (i) $Z = 5$ in $p_x + ip_y$ -wave junctions. a: $X = 0$ and b: $X = 0.9$.

in the p_x -wave case and is explained by the ZES. The increasing part is similar to that in the p_y -wave junctions. Since only a quasiparticle injected perpendicular to the interface contributes to the ZES, the effects of the spatial dependence of the pair potentials on the conductance are not negligible²⁸.

IV. SUMMARY

In this paper, we have calculated the polarization and temperature dependence of the zero-bias conductance

(ZBC) in F/I/S junctions, where we have chosen the symmetry of the pair potential as d -wave for high T_C cuprates and $p_x + ip_y$ -wave for Sr_2RuO_4 . As a reference, we have also studied the conductance in p_x and p_y -wave junctions. We have established a formalism of the ZBC which is available for the arbitrary θ_M which is the angle between the magnetization axis in ferromagnet and c -axis of superconductors. The θ_M dependence of the tunneling conductance only appears in the spin-triplet superconductor junctions. On the basis of the numerical results, we reach the following conclusions.

(1) When injected quasiparticles from ferromagnets always feel the zero-energy resonance state, *e.g.*, d -wave junction with (110) orientation and p_x -wave junction, the zero-bias tunneling conductance (ZBC) at the zero temperature is insensitive to the barrier potential at the interface. This property is useful for the determination of the degree of the spin-polarization in ferromagnets at sufficiently low temperatures. One of the promising candidate is $\text{LaSrMnO}/\text{YBaCuO}(\text{BiSrCaCuO})$ with well oriented (110) oriented interface. Within our theory, below 0.1K we can estimate the magnitude of polarization of ferromagnets through the value of the conductance of the junctions.

(2) For d -wave junctions with (110) orientation and p_x -wave junctions, the ZBC decreases with increasing temperatures when the degree of the polarization, X , is small. For large X , the ZBC is an increasing function of T . The presence of the ZES explains these behavior. In d -wave junctions with (100) orientation and p_y -wave junctions, the ZBC is an increasing function of T independent of X . This is because the ZES does not appear at these junction interface. For $p_x + ip_y$ -wave junctions, the ZBC first decreases with increasing T then increases.

(3) In p -wave junctions, the temperature dependence of the ZBC depends on the direction of the magnetization axis of ferromagnets because of the spin degree of freedom of Cooper pairs in spin-triplet superconductors.

(4) Throughout this paper, we have calculated the ZBC in two ways; i) the spatial dependence of the pair potential is assumed to be the step function (non-SCF calculation), ii) the spatial depletion of the pair potentials are determined self-consistently (SCF-calculation). We have confirmed that there are no remarkable differences between the conductance in the non-SCF calculation and those in the SCF calculation.

In this paper, effects of random potentials in ferromagnets are not taken into account. Recently, there are several works on random scattering effects in unconventional superconductor junctions^{68,69,70,71,72}. It is actually interesting to study transport properties of junctions where diffusive ferromagnets are attached to unconventional superconductors. In the present paper, the splitting of the ZBCP by magnetic fields through the Zeeman effect or magnetic impurities in an insulator are not taken into account^{40,41,42}. These are interesting and important future issues.

Acknowledgments

This work was partially supported by the Core Research for Evolutional Science and Technology (CREST)

of the Japan Science and Technology Corporation (JST). J.I. acknowledges support by the NEDO international Joint Research project "Nano-scale Magnetoelectronics".

-
- ¹ L. J. Buchholtz and G. Zwicknagl, *Phys. Rev. B* **23**, 5788 (1981).
- ² J. Hara and K. Nagai, *Prog. Theor. Phys.* **76**, 1237 (1986).
- ³ C. R. Hu, *Phys. Rev. Lett.* **72**, 1526 (1994).
- ⁴ S. Kashiwaya, Y. Tanaka, M. Koyanagi, H. Takashima and K. Kajimura, *Phys. Rev. B* **51**, 1350 (1995).
- ⁵ L. Alff, H. Takashima, S. Kashiwaya, N. Terada, H. Ihara, Y. Tanaka, M. Koyanagi and K. Kajimura, *Phys. Rev. B* **55** (1997) 14757.
- ⁶ M. Covington, M. Aprili, E. Paroanu, L.H. Greene, F. Xu, J. Zhu and C.A. Mirkin, *Phys. Rev. Lett.* **79**, 277 (1997).
- ⁷ J. Y. T. Wei, N.-C. Yeh, D. F. Garrigus, and M. Strasik, *Phys. Rev. Lett.* **81**, 2542 (1998).
- ⁸ W. Wang, M. Yamazaki, K. Lee, and I. Iguchi, *Phys. Rev. B* **60**, 4272 (1999).
- ⁹ I. Iguchi, W. Wang, M. Yamazaki, Y. Tanaka and S. Kashiwaya, *Phys. Rev. B* **62**, R6131 (2000).
- ¹⁰ Y. Tanaka and S. Kashiwaya, *Phys. Rev. B* **53**, 9371 (1996).
- ¹¹ Y. Tanaka and S. Kashiwaya, *Phys. Rev. B* **53**, 11957 (1996); **56**, 892 (1997); **58**, 2948 (1998).
- ¹² Y. Tanaka and S. Kashiwaya, *J. Phys. Soc. Jpn.* **68**, 3485 (1999); **69**, 1152 (2000).
- ¹³ Y. Asano, *Phys. Rev. B* **63**, 052512 (2001); *Phys. Rev. B* **64**, 014511 (2001); *J. Phys. Soc. Jpn.* **71**, 905 (2002).
- ¹⁴ Y. Tanuma, Y. Tanaka, M. Yamashiro and S. Kashiwaya, *Phys. Rev. B* **57**, 7997 (1998).
- ¹⁵ Y. Tanuma, Y. Tanaka, M. Ogata and S. Kashiwaya, *J. Phys. Soc. Jpn.*, **67**, pp.1118-1121, (1998).
- ¹⁶ Y. Tanuma, Y. Tanaka, M. Ogata and S. Kashiwaya, *Phys. Rev. B* **60**, 9817 (1999).
- ¹⁷ Y. Tanaka, T. Asai, N. Yoshida, J. Inoue and S. Kashiwaya, *Phys. Rev. B* **61**, R11902, (2000).
- ¹⁸ Y. Tanaka, Y. Tanuma and S. Kashiwaya, *Phys. Rev. B*, **64**, 054510, (2001).
- ¹⁹ Y. Tanaka, H. Tsuchiura, Y. Tanuma and S. Kashiwaya, *J. Phys. Soc. Jpn.* **71** 271, (2002).
- ²⁰ Y. Tanaka, H. Itoh, H. Tsuchiura, Y. Tanuma, J. Inoue, and S. Kashiwaya, *J. Phys. Soc. Jpn.* **71** 2005, (2002).
- ²¹ S. Ryu and Y. Hatsugai, *Phys. Rev. Lett.* **89** 077002 (2002).
- ²² Y. Tanaka and S. Kashiwaya, *Phys. Rev. Lett.* **74**, 3451 (1995).
- ²³ S. Kashiwaya, Y. Tanaka, M. Koyanagi, and K. Kajimura, *Phys. Rev. B* **53** 2667 (1996).
- ²⁴ S. Kashiwaya and Y. Tanaka, *Rep. Prog. Phys.* **63**, 1641 (2000).
- ²⁵ T. Löfwander, V. S. Shumeiko and G. Wendin, *Supercond. Sci. Technol.* **14**, R53 (2001).
- ²⁶ M. Yamashiro, Y. Tanaka, and S. Kashiwaya: *Phys. Rev. B* **56** (1997) 7847.
- ²⁷ M. Yamashiro, Y. Tanaka, Y. Tanuma and S. Kashiwaya, *J. Phys. Soc. Jpn.* **67**, 3224 (1998).
- ²⁸ M. Yamashiro, Y. Tanaka, N. Yoshida and S. Kashiwaya, *J. Phys. Soc. Jpn.* **68**, 2019 (1999).
- ²⁹ C. Honerkamp and M. Sigrist: *J. Low. Temp. Phys.* **111**, 898 (1998); *Prog. Theor. Phys.* **100**, 53 (1998).
- ³⁰ Y. Asano, *Phys. Rev. B* **64**, 224515 (2001).
- ³¹ Y. Tanaka, Y. Tanuma, K. Kuroki and S. Kashiwaya *J. Phys. Soc. Jpn.* **71** 2102 (2002).
- ³² Y. Tanaka, T. Hirai, K. Kusakabe and S. Kashiwaya, *Phys. Rev. B*, **60**, 6308 (1999).
- ³³ F. Laube, G. Goll, H. v. Löhneysen, M. Fogelström, and F. Lichtenberg, *Phys. Rev. Lett.* **84**, 1595 (2000).
- ³⁴ Z. Q. Mao, K. D. Nelson, R. Jin, Y. Liu, and Y. Maeno, *Phys. Rev. Lett.* **87**, 037003 (2001).
- ³⁵ C. Wälti, H. R. Ott, Z. Fisk, and J. L. Smith, *Phys. Rev. Lett.* **85**, 5258 (2000).
- ³⁶ K. Sengupta, I. Žutić, H.-J. Kwon, V.M. Yakovenko, and S. Das Sarma, *Phys. Rev. B* **63**, 144531 (2001).
- ³⁷ Y. Tanuma, K. Kuroki, Y. Tanaka, and S. Kashiwaya, *Phys. Rev. B* **64**, 214510 (2001).
- ³⁸ Y. Tanuma, K. Kuroki, Y. Tanaka, R. Arita, S. Kashiwaya and H. Aoki, *Phys. Rev. B* **66** 094507 (2002).
- ³⁹ A. F. Andreev, *Zh. Eksp. Teor. Fiz.* **46**, 1823 (1964). [*Sov. Phys. JETP* **19**, 1228 (1964).]
- ⁴⁰ J. X. Zhu, B. Friedman, and C. S. Ting, *Phys. Rev. B* **59**, 9558 (1999).
- ⁴¹ S. Kashiwaya, Y. Tanaka, N. Yoshida, and M. R. Beasley, *Phys. Rev. B* **60**, 3572 (1999).
- ⁴² I. Zutic and O. T. Valls, *Phys. Rev. B* **60**, 6320 (1999); **61**, 1555 (2000).
- ⁴³ N. Yoshida, Y. Tanaka, J. Inoue, and S. Kashiwaya, *J. Phys. Soc. Jpn.* **68**, 1071 (1999).
- ⁴⁴ N. Stefanakis, *Phys. Rev. B* **64**, 224502 (2001); *J. Phys. Cond. Matt.* **13**, 3643 (2001).
- ⁴⁵ T. Hirai, N. Yoshida, Y. Tanaka, J. Inoue, and S. Kashiwaya, *J. Phys. Soc. Jpn.* **70**, 1885 (2001).
- ⁴⁶ T. Hirai, N. Yoshida, Y. Tanaka, J. Inoue and S. Kashiwaya, *Physica C* **367** 137 (2002).
- ⁴⁷ A. Buzdin, *Phys. Rev. B* **62** 11377 (2000).
- ⁴⁸ G. Y. Sun, D. Y. Xing, J. M. Dong, M. Liu, *Phys. Rev. B* **65** 174508 (2002).
- ⁴⁹ Z. C. Dong, D. Y. Xing, and J. Dong *Phys. Rev. B* **65**, 214512 (2002)
- ⁵⁰ N. Yoshida, H. Itoh, H. Tsuchiura, Y. Tanaka, J. Inoue, and S. Kashiwaya, *Physica C* **367** 185 (2002)
- ⁵¹ N. Yoshida, H. Itoh, T. Hirai, Y. Tanaka, J. Inoue, and S. Kashiwaya, *Physica C* **367**, 165 (2002).
- ⁵² Z. Y. Chen, A. Biswas, I. Zutic, T. Wu, S. B. Ogale, R. L. Greene, and T. Venkatesan, *Phys. Rev. B* **63**, 212508 (2001).
- ⁵³ A. Sawa, S. Kashiwaya, H. Obara, H. Yamasaki, M. Koyanagi, Y. Tanaka and N. Yoshida, *Physica C Vol.* **339**, 107, 2000
- ⁵⁴ H. Kashiwaya, A. Sawa, S. Kashiwaya, H. Yamazaki, M. Koyanagi, I. Kurosawa, Y. Tanaka, and I. Iguchi, *Physica C* **357-360** 1610 (2001).
- ⁵⁵ C.-C. Fu, Z. Huang, and N.-C. Yeh *Phys. Rev. B* **65**, 224516 (2002)

- ⁵⁶ Y. Nagato and K. Nagai, Phys. Rev. B **51** 16254 (1995).
- ⁵⁷ M. Matsumoto and H. Shiba, J. Phys. Soc. Jpn. **64** 3384 (1995), **64** 4867, **65** 2194 (1995).
- ⁵⁸ Y. Ohashi, J. Phys. Soc. Jpn. **65**, 823 (1996).
- ⁵⁹ A. Millis, D. Rainer, and J. A. Sauls, Phys. Rev. B **38**, 4504 (1988).
- ⁶⁰ C. Bruder, Phys. Rev. B. **41**, 4017 (1990).
- ⁶¹ G. E. Blonder, M. Tinkham, and T. M. Klapwijk, Phys. Rev. B **25**, 4515 (1982).
- ⁶² A. V. Zaitsev, Zh. Eksp. Teor. Fiz. **86**, 1742 (1984); Engl. Transl. Sci. Phys.-JETP (1015) **59**.
- ⁶³ A. L. Shelankov, J. Low. Temp. Phys. **60**, 29 (1985).
- ⁶⁴ M. Ashida, S. Aoyama, J. Hara, and K. Nagai, Phys. Rev. **40**, 8673 (1989).
- ⁶⁵ Y. Nagato, K. Nagai, and J. Hara, J. Low Tem. Phys. **93**, 33 (1993).
- ⁶⁶ T. Hirai, Y. Tanaka, and J. Inoue, unpublished.
- ⁶⁷ Y. Tanuma, Y. Tanaka, and S. Kashiwaya, Rhys. Rev. B **64**, 214519 (2001).
- ⁶⁸ H. Itoh, Y. Tanaka, J. Inoue and S. Kashiwaya Physica C **367** pp. 99-102 (2002).
- ⁶⁹ Y. Asano and Y. Tanaka, Phys. Rev. B **65** 064522 (2002).
- ⁷⁰ Y. Tanaka, Y. Nazarov and S. Kashiwaya, unpublished.
- ⁷¹ N. Yoshida, Y. Asano, H. Itoh, Y. Tanaka, J. Inoue and S. Kashiwaya, J. Phys. Soc. Jpn. (2003).
- ⁷² The present model deals with the ideal situation where the height of the ZBCP is only the function of the polarization of the ferromagnet. However, in real junctions, the interface quality and the impurity distribution near the interface may have influences on the ZBCP height. Detailed analysis of such factors will be discussed in coming papers.